

Phase stability and pyroelectricity of antiferroelectric PLZST oxide

Wai-Hung Chan · Zhengkui Xu · Jiwei Zhai · Eugene V. Colla · Haydn Chen

Published online: 23 March 2007
© Springer Science + Business Media, LLC 2007

Abstract Polarization and transmission electron microscopy studies of the $\text{Pb}_{0.97}\text{La}_{0.02}(\text{Zr}_{0.65}\text{Sn}_{0.22}\text{Ti}_{0.13})\text{O}_3$ (PLZST) ceramics confirmed the antiferroelectric (AFE) nature of this material. The electric-field-induced ferroelectric (FE) phase has a lifetime much longer than the reasonable laboratory time scale at $T \leq 60^\circ\text{C}$. The observed frequency dispersion of the dielectric constant reflects the competition between AFE and FE orderings. At high temperatures, the induced-FE phase reverses fast to the AFE phase. This process produces a pronounced pyroelectric current. The FE-to-AFE transition temperature can also be tuned by a dc bias field.

Keywords Antiferroelectric · PLZST ceramics · Pyroelectric properties · Frequency dispersion · Tunability

1 Introduction

Antiferroelectric (AFE) materials are characterized by the anti-parallel alignment of dipoles, which results in zero net

spontaneous polarization. The application of the electric field higher than a critical switching field ($E_{\text{AFE-FE}}$) to the AFE material will break the anti-parallel alignment and the parallel dipole alignment similar to the FE can be achieved. After removal of the field, the induced FE state reverses to the low-energy AFE phase very quickly. During the FE–AFE back switching, the stored polarization is released and a very high current is produced. In this article, we report the results obtained from AFE lead lanthanum zirconate stannate titanate of a nominal composition $\text{Pb}_{0.97}\text{La}_{0.02}(\text{Zr}_{0.65}\text{Sn}_{0.22}\text{Ti}_{0.13})\text{O}_3$, where the field-induced FE phase was found to be very stable at $T \leq 60^\circ\text{C}$. The FE–AFE switching characteristics are temperature dependent and this material is suitable for uncooled heat sensing applications, which has never been reported before. To understand the phase stability of this material, the optimal poling conditions and the role of dc bias field were also investigated.

2 Experimental procedure

PLZST ceramics were fabricated using a mixed-oxide method and the processing details can be found elsewhere [1]. The phases present in the ceramics were identified by x-ray diffraction (XRD), whereas the microstructure was examined using Philip CM20 transmission electron microscopy (TEM) equipped with a hot stage. Selected area electron diffraction (SAED) patterns along [001] direction were recorded at different temperatures. For the measurements of the electrical properties, the gold electrodes were deposited by dc sputtering. The polarization versus electric field (P–E) hysteresis loops were measured using a Radiant Technologies Precision Pro ferroelectric tester. Pyroelectric properties were studied by HP4140B picoammeter using

W.-H. Chan · Z. Xu (✉) · J. Zhai · E. V. Colla · H. Chen
Department of Physics and Materials Science,
City University of Hong Kong, Kowloon, Hong Kong
e-mail: apzkk@cityu.edu.hk

E. V. Colla
Department of Physics,
University of Illinois at Urbana-Champaign,
Urbana, IL 61801, USA

H. Chen
Department of Physics, Tunghai University,
Taichung 407, Taiwan

the Byre and Roundy direct technique [2]. The Agilent 4284A LCR meter was used for dielectric constant measurements. All electrical measurements were done as a function of temperature in the computer controlled chamber (Delta 9023).

3 Results and discussion

The crystalline perovskite structure of PLZST ceramic was confirmed by XRD (data not shown here). The phase transformation behavior of this material was analyzed by the P–E measurements. Two hysteresis loops per six distinct temperatures of 20, 60, 85, 100, 135, and 200°C are depicted in Fig. 1(a–f), respectively. The first loop (1) in each figure was taken from a virgin sample (cooled from 300°C to the measuring temperature in a zero field), whereas the second loop (2) was immediately taken after the first one. The scanning time in all P–E experiments was 100 ms. At 20°C [Fig. 1(a)], the first P–E loop started from the origin and had a small slope (dP/dE), which was consistent with the typical AFE behavior. Then a step-like transition from AFE to the FE state was observed at ~ 2 kV/mm, which corresponds to the $E_{\text{AFE-FE}}$. Afterward the system displayed a nearly rectangular FE hysteresis loop (2) with a coercive field (E_C) of ~ 1 kV/mm and remanent polarization of $\sim 31 \mu\text{C}/\text{cm}^2$. Similar P–E behaviors with

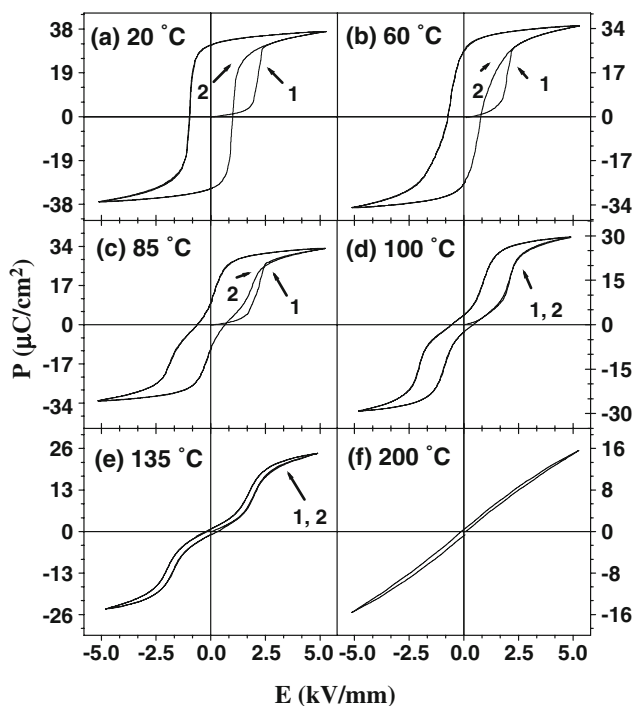


Fig. 1 Two consecutive hysteresis loops taken at (a) 20, (b) 60, (c) 85, (d) 100, (e) 135, and (f) 200°C. Loop 1—at virgin sample; Loop 2—the second run

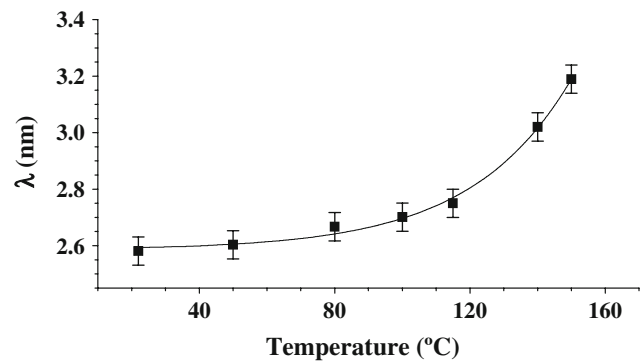


Fig. 2 Modulation wavelength (λ) as a function of temperature for PLZST ceramics

$E_{\text{AFE-FE}} > E_C$ could still be observed at the temperatures up to $\sim 90^\circ\text{C}$ [Fig. 1(b, c)]. However, at $T > 90^\circ\text{C}$ the typical AFE double hysteresis loops (both the first and the second) are evident from Fig. 1(d, e). A similar behavior was observed in $\text{Pb}_{0.97}\text{La}_{0.02}(\text{Zr}_{0.60}\text{Sn}_{0.30}\text{Ti}_{0.10})\text{O}_3$ ceramics [1, 3]. It is believed that the ground state of PLZST at $20 \leq T < 100^\circ\text{C}$ is AFE instead of FE as previously claimed by Berlincourt [4]. However, for this particular temperature range the application of the electrical field can induce a FE phase with characteristic lifetime longer than the measuring time. On the other hand, the recovery to the AFE state is fast at high temperatures, which leads to the typical AFE double P–E behavior. Further evidence in favor of the AFE nature of this material system at $T \geq 20^\circ\text{C}$ is provided by the TEM studies. Incommensurate $1/x < 110 >$ superlattice spots were observed at $20 \leq T < 170^\circ\text{C}$ from the [001] SAED patterns. AFE structural modulation wavelengths (λ) calculated from the reciprocal separation distances between the superlattice spots and the relevant main reflections along $< 110 >$ direction at various temperatures are depicted in Fig. 2. When the temperature was increased to above 160°C , no AFE incommensurate superlattice spots could be detected and the linear polarization behavior became evident [Fig. 1(f)], suggesting a simple cubic paraelectric state at high temperatures.

After poling the sample in different dc electric fields (1–5 kV/mm) at $\sim 20^\circ\text{C}$ for 10 min, a current peak was observed upon heating. This is attributed to an abrupt change in polarization during FE–AFE switching, which modulates the surface electric charge and produces a pyroelectric current through a capacitor of surface A [5]

$$I = A(dD/dt) = A(dD/dT)(dT/dt) = Ap(dT/dt), \quad (1)$$

where t is time, D is dielectric displacement, T is absolute temperature and p is conventional pyroelectric coefficient. Pyroelectric coefficients calculated from the measured pyroelectric currents through Eq. (1) are displayed in Fig. 3. The pyroelectric coefficient peak temperature, which

is associated with the FE-to-AFE transition, is $\sim 60^\circ\text{C}$ for the studied PLZST ceramics and is independent of the magnitude of the poling field. However, the magnitude of pyroelectric coefficient maximum increases and the full-width-half-maximum of this peak decreases with increasing poling field from 1.00 to 4.21 kV/mm. Further increase of the poling field did not have any pronounced effect on pyroelectric coefficient maximum. The poling treatment for this material described in the following sections was done with a field of 4.21 kV/mm at room temperature. It is also interesting to note that the FE-to-AFE transition temperature ($T_{\text{FE-AFE}}$) did not change after storing the poled sample at room temperature for 2 weeks. It remains in the induced-FE state at $T < T_{\text{FE-AFE}}$, as confirmed by the P–E behavior depicted in Fig. 3(a). This result indicates that the induced FE phase has a lifetime exceeding the reasonable laboratory time scale at low temperatures. The PLZST could return to its original AFE state only when the temperature was high enough [Fig. 3(b, c)].

All our experimental data suggest that the ground state of the studied system is AFE, but AFE alignment is very fragile and can be easily destroyed by the application of an electric field. This results in the appearance of an induced FE phase having very long relaxation time back to AFE state. In Fig. 4, a strong frequency dispersion of the dielectric constant is observed below 100°C . It may arise from the competition between the FE and the AFE interaction, which creates a state of frustration similar to dipole glass or spin glass. Similar frequency relaxation has also been reported for AFE $\text{Pb}_{0.97}\text{La}_{0.02}(\text{Zr}_{0.60}\text{Sn}_{0.30}\text{Ti}_{0.10})\text{O}_3$ ceramics at low temperatures, where temporal FE behavior was observed [3].

The pyroelectric properties of the poled PLZST ceramics under various dc bias fields upon heating were also studied.

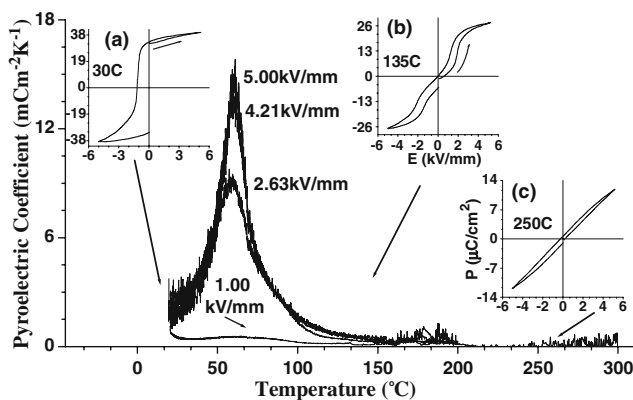


Fig. 3 Temperature dependence of pyroelectric coefficient of the PLZST ceramics after poling with the field of 1.00, 2.63, 4.21, or 5.00 kV/mm at 20°C . The inserts represent the hysteresis loops taken at (a) 30, (b) 135, and (c) 250°C after poling with the field of 4.21 kV/mm and then aging without field at 20°C for 2 weeks

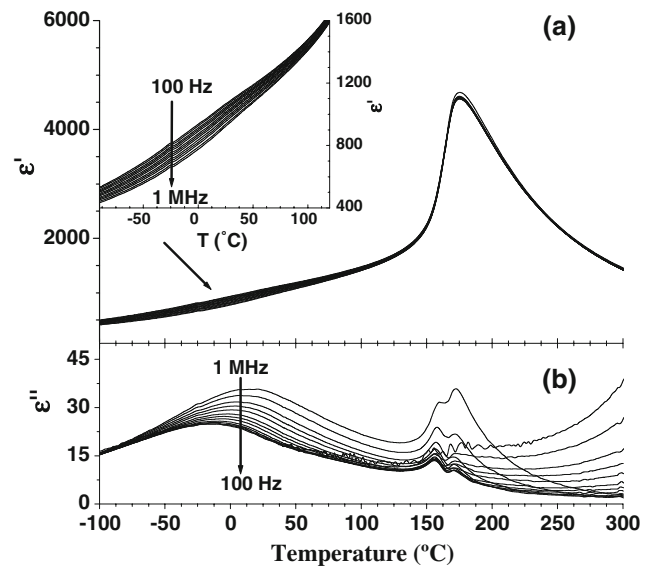


Fig. 4 (a) The real and (b) imaginary parts of the dielectric constant as a function of temperature for various frequencies. The insert represents the real part of dielectric constant below 120°C

The shifting of the FE-to-AFE phase transition temperature with dc bias field is illustrated in Fig. 5. The shifting is $\sim 39^\circ\text{C kV}^{-1} \text{ mm}^1$ and very large compared with the data reported by Yang *et al* [6]. Moreover, it was found that the magnitude of pyroelectric coefficient maximum is of the order of 10^{-3} – $10^{-2} \text{ Cm}^{-2} \text{ K}^{-1}$ and larger than those for some important pyroelectric materials such as lead zirconate titanate ($380 \mu\text{Cm}^{-2} \text{ K}^{-1}$) and lithium tantalite crystal ($230 \mu\text{Cm}^{-2} \text{ K}^{-1}$) [7]. The outstanding pyroelectric coefficient and the high ability to adjust the working temperature make PLZST attractive for the application of uncooled electric field tunable thermal sensor.

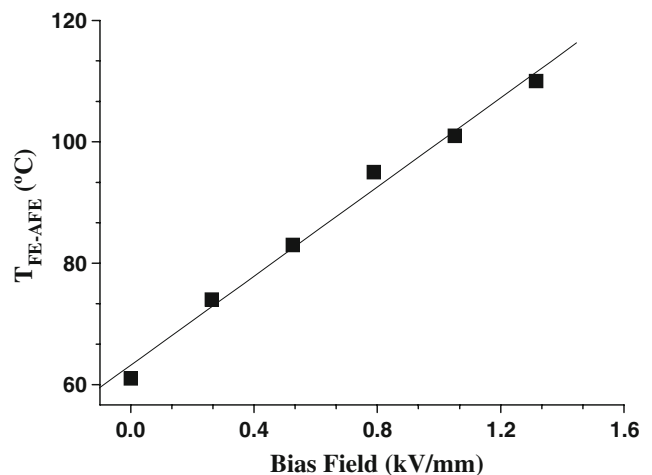


Fig. 5 Ferroelectric-to-antiferroelectric transition temperature ($T_{\text{FE-AFE}}$) versus dc bias field

4 Conclusions

Transmission electron microscopy and polarization studies confirmed the AFE nature of the $\text{Pb}_{0.97}\text{La}_{0.02}(\text{Zr}_{0.65}\text{Sn}_{0.22}\text{Ti}_{0.13})\text{O}_3$ ceramics at $T < 170^\circ\text{C}$, which is in disagreement with the published lead lanthanum zirconate stannate titanate ternary phase diagram. The electric-field-induced ferroelectric exhibited an unusual high stability, which was independent of the laboratory measuring time scale. Upon zero field heating, the poled sample transformed back to its original AFE state at $\sim 60^\circ\text{C}$. This transformation accompanied by a pyroelectric current peak and the peak temperature could be adjusted by a dc bias. The record-high magnitude of the pyroelectric coefficient and outstanding dc tunability make this material attractive for fabricating uncooled tunable pyroelectric thermal sensors.

Acknowledgments The work described in this paper was jointly supported both by a grant from the Research Grants Council of the Hong Kong Special Administrative Region, China (Project No. 9360083) and a grant from City University of Hong Kong (Project No. 7001464). One of the authors (HC) also wishes to acknowledge the support from the Tunghai University for the completion of data analysis and manuscript preparation.

References

1. W.-H. Chan, Z. Xu, Y. Zhang, T.F. Hung, H. Chen, *J. Appl. Phys.* **94**, 4563 (2003)
2. R.L. Byer, C.B. Roundy, *Ferroelectrics* **3**, 333 (1972)
3. W.-H. Chan, Haydn Chen, E.V. Colla, *Appl. Phys. Lett.* **82**, 2314 (2003)
4. D. Berlincourt, *IEEE Trans. Sonics Ultrason.* **SU-13**, 116 (1966)
5. A. Amin, *J. Electroceram.* **8**, 99 (2002)
6. T. Yang, P. Liu, Z. Xu, L. Zhang, X. Yao, *Ferroelectrics* **230**, 181 (1999)
7. S. Bauer, B. Ploss, *J. Appl. Phys.* **68**, 6361 (1990)